

Polarization sensitive anisotropic structuring of silicon by ultrashort light pulses

Jingyu Zhang, Rokas Drevinskas, Martynas Beresna, and Peter G. Kazansky

Citation: [Applied Physics Letters](#) **107**, 041114 (2015); doi: 10.1063/1.4928043

View online: <http://dx.doi.org/10.1063/1.4928043>

View Table of Contents: <http://scitation.aip.org/content/aip/journal/apl/107/4?ver=pdfcov>

Published by the [AIP Publishing](#)

Articles you may be interested in

[Polarization sensitivity of light diffraction for periodic array of anisotropic gold nanoparticles](#)

Appl. Phys. Lett. **106**, 241107 (2015); 10.1063/1.4922808

[Nuclear spin polarization induced by ultrashort laser pulses](#)

AIP Conf. Proc. **915**, 996 (2007); 10.1063/1.2750942

[Phase-sensitive interferometry with ultrashort optical pulses](#)

Rev. Sci. Instrum. **66**, 5459 (1995); 10.1063/1.1146069

[Ultrashort light pulses](#)

Rev. Sci. Instrum. **60**, 3597 (1989); 10.1063/1.1140516

[Generation and Measurement of Ultrashort Light Pulses](#)

J. Appl. Phys. **39**, 6041 (1968); 10.1063/1.1656112

The logo for AIP APL Photonics is displayed in a white font on a red background. The letters 'AIP' are large and bold, followed by a vertical bar and the words 'APL Photonics' in a smaller font.

APL Photonics is pleased to announce
Benjamin Eggleton as its Editor-in-Chief



Polarization sensitive anisotropic structuring of silicon by ultrashort light pulses

Jingyu Zhang, Rokas Drevinskas,^{a)} Martynas Beresna, and Peter G. Kazansky
Optoelectronics Research Centre, University of Southampton, Southampton SO17 1BJ, United Kingdom

(Received 26 May 2015; accepted 24 July 2015; published online 29 July 2015)

Imprinting of anisotropic structures on the silicon surface by double pulse femtosecond laser irradiation is demonstrated. The origin of the polarization-induced anisotropy is explained in terms of interaction of linearly polarized second pulse with the wavelength-sized symmetric crater-shaped structure generated by the linearly polarized first pulse. A wavefront sensor is fabricated by imprinting an array of micro-craters. Polarization controlled anisotropy of the structures can be also explored for data storage applications. © 2015 AIP Publishing LLC.

[<http://dx.doi.org/10.1063/1.4928043>]

It is well recognized that tightly focused ultrafast laser pulses can produce localized structural modifications with the precision of tens of nanometers.^{1,2} Consequently, femtosecond laser assisted imprinting has been exploited for implementing a high capacity multi-dimensional optical data storage,³ fabrication of polarization sensitive elements,⁴ micro-fluidic channels,⁵ and waveguides.⁶ The interaction of ultrashort light pulses with materials is defined by multiple parameters, among which polarization plays a significant roles.⁷ In particular, the formation of polarization dependent self-assembled periodic nanostructures is commonly observed, either within bulk^{8–11} or on surface,^{12,13} in the experiments of ultrafast laser direct writing. Another manifestation of the polarization is the anisotropy of near-field distribution produced by the interaction of linearly polarized beam with sub-wavelength structures, which can be revealed via imprinting in photosensitive polymer¹⁴ or ablation of gold nanoparticles.¹⁵ In this letter, we report the polarization sensitive writing with femtosecond double pulse irradiation on the silicon surface. We demonstrate the imprinting of anisotropic near-field pattern, which is produced by the interaction of the linearly polarized second pulse with a symmetric wavelength scale structures generated by the linearly polarized first pulse. The experimental results are supported by numerical simulations of near-field anisotropy of linearly polarized light distribution. We also demonstrate the application of structures imprinted on silicon surface by a single pulse for wavefront sensor fabrication.

Experiments were performed using a mode-locked Yb:KGW ultrafast laser system (Pharos, Light Conversion Ltd.) operating at a wavelength of 1030 nm, 20 kHz repetition rate, and 330 fs pulse duration. Series of dots were printed on the surface of p-type crystalline silicon (111) substrate by either single or double pulse (50 μ s time delay between pulses) irradiation with a linear polarization controlled by a zero-order half-wave plate. The laser beam was focused via a 0.65 NA objective lens in the range from 0 to 12 μ m above the surface. The pulse energy was varied up to 300 nJ in order to depict a large modification window.

^{a)}Author to whom correspondence should be addressed. Electronic mail: rd1c12@orc.soton.ac.uk

After laser irradiation, the morphological changes of the surface were characterized using an optical microscope (BX51 Olympus, Inc.), scanning electron microscope (SEM) (Zeiss Evo50), and atomic force microscope (AFM) (Nanonics Multiview 2000).

A smooth and symmetric 150 nm deep crater-shaped structure with a rim was observed after focusing a single 120 nJ (1.35 J/cm²) pulse 4 μ m above the silicon surface (Figs. 1(a)–1(d)). The crater's radius of curvature of $2.69 \pm 0.08 \mu$ m was estimated from AFM profiles (Fig. 1(c)). Material ejection was not observed at these pulse energies; thus, we assume the structure was formed by a rarefaction (shock) wave, which pushed the molten material from the center to the periphery of the irradiated zone.¹⁶ The light was absorbed by electrons, which afterwards transferred energy to the lattice via electron-phonon coupling resulting in an isotropic heating zone without any collateral damage.¹⁷ During the irradiation with the first pulse, substrate's surface was flat and homogeneous leading to an isotropic near-field distribution. No asymmetry was observed in the crater-shaped structures induced by a single pulse at any of six different orientations of linear polarization.

The isotropic crater structures with their smooth surface can be implemented as a mold for microlens fabrication or itself can be employed as an optical microreflector with a focal length of $1.345 \pm 0.04 \mu$ m (Fig. 1(c)). To demonstrate this, the sample was examined under an optical microscope in the reflection mode, when the illumination was partly blocked by an aperture. While moving the focal position of the microscope objective, we could clearly see the rectangular aperture imaged by the microreflector (Fig. 1(d)). The array of 5×5 microreflectors was imprinted on the silicon surface (Fig. 2) and implemented as a wavefront sensor.¹⁸ After examining the shape of each crater shown in Fig. 2(a), the position of the geometrical focus was estimated. Tracking the lateral displacement of the imaged aperture (Fig. 2(b)), the map indicating the wavefront of illumination was extracted (Fig. 2(c)).

Unexpectedly, we observed a completely different modification with the double pulse structuring of the sample. Here, an anisotropic transformation of the modified region was observed with the formation of several peculiar features (Figs. 1(e)–1(h)). First, in the middle part of the crater, two enhanced modification zones oriented perpendicular to the

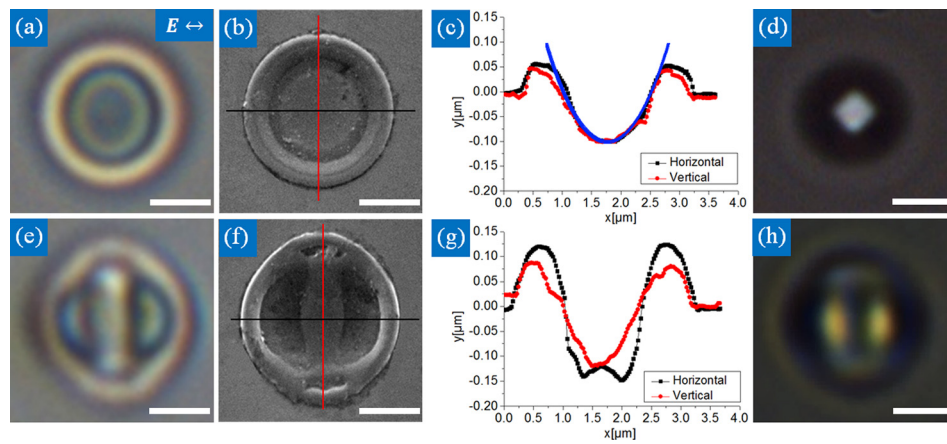


FIG. 1. Silicon structures induced by linearly polarized single pulse (a)–(d) and double pulse (e)–(h) femtosecond laser irradiation. (a) and (e) Optical reflection and (b) and (f) topological SEM images, as well as (c) and (g) AFM profile scans were performed after the first and second pulses; the blue line is the fitting curve for the surface curvature with $R = 2.7 \mu\text{m}$. Pulses with the energy of 120 nJ were focused $4 \mu\text{m}$ above the silicon surface (1.35 J/cm^2). E indicates the polarization state of the pulse. The images in (d) and (h) represent the microscope aperture imaged using the laser-induced structures shown in (a) and (e), respectively. The scale bars: $1 \mu\text{m}$.

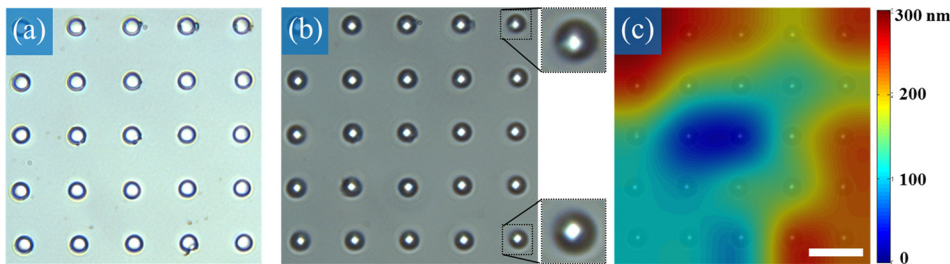


FIG. 2. Silicon microreflectors array induced by single femtosecond laser pulses. Optical reflection images were taken (a) without and (b) with microscope aperture inserted in front of the illumination source. (c) The focal point displacement map caused by the wavefront of illumination was extracted from (a) and (b) images. The scale bar is $10 \mu\text{m}$.

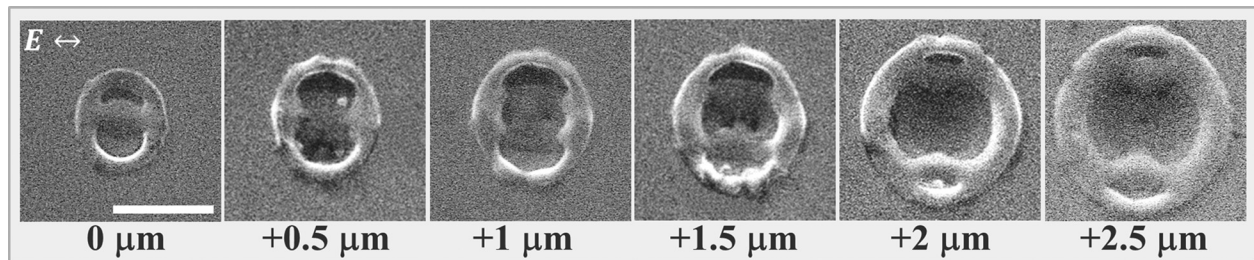


FIG. 3. SEM images of the linearly polarized double pulse modification induced at different focusing positions varying from $0 \mu\text{m}$ to $2.5 \mu\text{m}$ above the surface. The pulse energy was fixed at 15 nJ ($0.27\text{--}0.47 \text{ J/cm}^2$). Scale bar is $1 \mu\text{m}$.

light polarization were induced. As a result, a bridge-like structure with a height of roughly 25 nm was formed (Figs. 1(e)–1(g)). The orientation of the bridge was perpendicular to the polarization and located in the center of the modified region (Fig. 1(e)). Second, the rim was deformed at the tips of the bridge slightly elongating the crater shape (Fig. 1(f)). The crater depth along the direction parallel to the beam polarization was increased by more than 80%, while along the perpendicular direction only by 30% (Fig. 1(g)). The two induced lobes located inside the crater were functioning as twin microreflectors (Fig. 1(h)).

The shape of the structure was changing significantly when the laser beam was defocused (Fig. 3). The bridge was either merging or separating depending on the beam focal position. If the double pulse laser beam was focused on the surface, the bridge-shape structure oriented parallel to the polarization direction was produced (Fig. 3, left), whereas the structure similar to the one in Fig. 1(f) emerged when the

focus of the beam was above the sample surface (Fig. 3, right).

The wavelength-sized polarization sensitive structures on silicon surface may find applications for the polarization-multiplexed optical memory. The size and orientation of the structure can be independently manipulated by the energy of

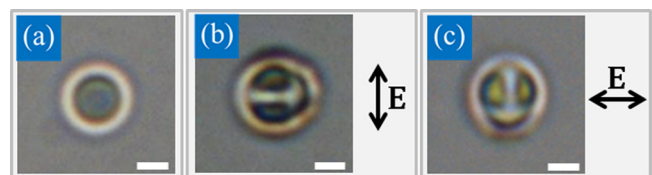


FIG. 4. Optical microscope images of the silicon surface modified with (a) single and (b) and (c) writing pulses with two different polarizations indicated by arrows. Pulses with the energy of 40 nJ (0.77 J/cm^2) were focused at $2.5 \mu\text{m}$ above the surface. The scale bars: $1 \mu\text{m}$.

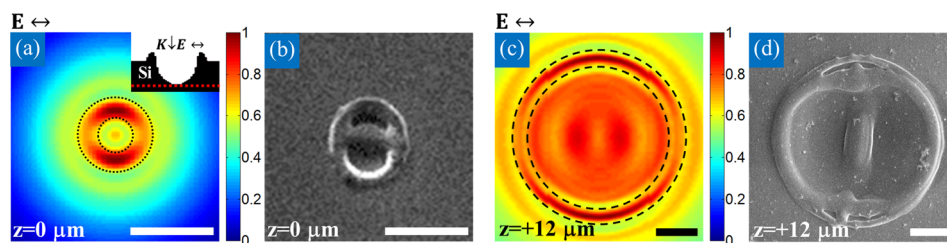


FIG. 5. (a) and (c) Calculated total electric near-field distribution of the light propagating through an isotropic crater-shape silicon structure, and (b) and (d) its subsequent polarization sensitive modification measured by SEM. The double pulse laser beam was focused at (a) and (b) $0\ \mu\text{m}$ and (c) and (d) $12\ \mu\text{m}$ above the substrate surface with the pulse energies of $15\ \text{nJ}$ ($0.47\ \text{J}/\text{cm}^2$) and $300\ \text{nJ}$ ($0.55\ \text{J}/\text{cm}^2$), respectively. The dashed black lines in (a) and (c) indicate the contours of crater-shape pattern used for the calculations. Insets in (a) show the geometry of the pattern used to mimic the conditions during the second pulse irradiation. The dashed red lines—planes of the near-field monitoring. The scale bars: $1\ \mu\text{m}$.

the first pulse and polarization of the second pulse, respectively. Assuming that the shorter wavelength should produce proportionally smaller structures with the same polarization dependence, we estimated that by recording data with wavelength of $300\ \text{nm}$, a CD-sized disc with the capacity of $36\ \text{GB}$ can be achieved ($0.5\ \mu\text{m}$ between track pitches, 6 bits polarization-multiplexed data resulting from 64 polarization states between 0° and 180° , and 2 bits power-multiplexed data per structure). The read-out technology could be implemented by monitoring the intensity of the linearly polarized laser beam, when the reflected light is modulated (Fresnel conditions) by the surface morphology. The modulation in intensity and polarization could be detected using a quadrupole detector, which is already exploited in the traditional optical data storage read-out.

In addition, experiments were performed to demonstrate the multilevel polarization sensitive encoding on silicon surface (Fig. 4). First of all, the isotropic craters were imprinted by the single pulse irradiation (Fig. 4(a)). Later, during the encoding stage, the subsequent irradiation with different states of polarization of the writing beam was used to control the orientation of anisotropy of the imprinted structures (Figs. 4(b) and 4(c)). The slight asymmetry of the patterns in the direction perpendicular to the polarization could be explained by the displacement of the focal spot during the polarization rotation.

For the theoretical analysis, the corresponding total near-field distribution was obtained simulating the propagation of the focused second pulse through a symmetric crater-shape structure pre-defined by the first pulse (Fig. 5). A commercial-grade simulator (Lumerical) based on the finite-difference time-domain (FDTD) method was used to perform the numerical calculations of a total near-field distribution. Here, we distinguish between two regimes of polarization dependence for the light propagating through a large size ($d > \lambda$) and a subwavelength size ($d < \lambda$) single circular crater. We can assume that such a structure in the near-field behaves as an aperture. In this case, the explanation may be applied on the basis of an anisotropic near-field distribution dominated for different regions of structure within the surface-wave modes and the field coupling to the wave-guided modes of the aperture.¹⁹ For all conditions, two sets of the lobes of an intense field localized under the rim of the structure are generated with the orientation parallel to the light polarization (Figs. 5(a) and 5(c)). The generated mode

in the center of the structure almost vanishes when the crater size is smaller than the excitation wavelength ($d/\lambda = 0.9$) (Fig. 5(a)). Then the strong field generated inside the rim region dominates (Fig. 5(a)). In such a system, it is expected to have a modification localized at the edges of the crater and oriented parallel to the field polarization. When the crater size increases ($d/\lambda = 4.0$), the lobes generated inside the rim are accompanied by the series of perpendicular lobes generated in the central part of the crater (Fig. 5(c)).

The FDTD simulated field patterns (Figs. 5(a) and 5(c)) are in a good agreement with the morphology of re-solidified material (Figs. 5(b) and 5(d)) observed experimentally. Indeed, under the focusing conditions when the modification area is smaller than the laser wavelength, the symmetric structure is slightly elongated, and the bridge-like structure along the polarization is produced (Fig. 5(b)). On the other hand, the bridge-like structure perpendicular to the polarization occurs when the beam is defocused (Fig. 5(d)). At the same time, the regions of the rim perpendicular to the bridge are modified, matching the intensity distribution visualized in numerical analysis (Fig. 5(c)).

In conclusion, we have experimentally demonstrated the polarization sensitive structuring on a silicon surface by the linearly polarized femtosecond double pulses. The distribution of electric near-field becomes asymmetric and polarization dependent when the second pulse propagates through a circular crater structure produced by the first pulse. The phenomenon enables imprinting of optical microreflectors within the single pulse irradiation and is exploited for demonstrating the direct mapping of the near-field distribution within multi-pulse experiments. Polarization sensitive structuring on silicon can be used for the security marking or data storage applications.

This work was supported by the UK Physical Sciences Research Council (EPSRC).

¹E. N. Glezer, M. Milosavljevic, L. Huang, R. J. Finlay, T.-H. Her, J. P. Callan, and E. Mazur, *Opt. Lett.* **21**, 2023 (1996).

²A. P. Joglekar, H. Liu, G. J. Spooner, E. Meyhöfer, G. Mourou, and A. J. Hunt, *Appl. Phys. B: Lasers Opt.* **77**, 25–30 (2003).

³J. Zhang, M. Gecevičius, M. Beresna, and P. G. Kazansky, *Phys. Rev. Lett.* **112**, 033901 (2014).

⁴M. Beresna, M. Gecevičius, and P. G. Kazansky, *Opt. Mater. Express* **1**, 783 (2011).

⁵Y. Bellouard, A. Said, M. Dugan, and P. Bado, *Opt. Express* **12**, 2120 (2004).

- ⁶K. Miura, J. Qiu, H. Inouye, T. Mitsuyu, and K. Hirao, *Appl. Phys. Lett.* **71**, 3329 (1997).
- ⁷P. Kazansky, H. Inouye, T. Mitsuyu, K. Miura, J. Qiu, K. Hirao, and F. Starrost, *Phys. Rev. Lett.* **82**, 2199 (1999).
- ⁸B. Pommellec, M. Lancy, A. Cahid-Erraji, and P. G. Kazansky, *Opt. Mater. Express* **1**, 766–782 (2011).
- ⁹Y. Shimotsuma, P. G. Kazansky, J. Qiu, and K. Hirao, *Phys. Rev. Lett.* **91**, 247405 (2003).
- ¹⁰J. Gottmann, D. Wortmann, and M. Hörstmann-Jungemann, *Appl. Surf. Sci.* **255**, 5641 (2009).
- ¹¹V. Bhardwaj, E. Simova, P. Rajeev, C. Hnatovsky, R. Taylor, D. Rayner, and P. Corkum, *Phys. Rev. Lett.* **96**, 057404 (2006).
- ¹²J. Bonse, J. Krüger, S. Höhm, and A. Rosenfeld, *J. Laser Appl.* **24**, 042006 (2012).
- ¹³R. Drevinskas, M. Beresna, M. Gecevičius, M. Khenkin, A. G. Kazanskii, I. Matulaitienė, G. Niaura, O. I. Konkov, E. I. Terukov, Yu. P. Svirko, and P. G. Kazansky, *Appl. Phys. Lett.* **106**, 171106 (2015).
- ¹⁴F. H'dhili, R. Bachelot, G. Lerondel, D. Barchiesi, and P. Royer, *Appl. Phys. Lett.* **79**, 4019 (2001).
- ¹⁵A. Plech, V. Kotaidis, M. Lorenc, and J. Boneberg, *Nat. Phys.* **2**, 44 (2006).
- ¹⁶A. Borowiec, M. MacKenzie, G. C. Weatherly, and H. K. Haugen, *Appl. Phys. A: Mater. Sci. Process.* **76**, 201 (2003).
- ¹⁷S. K. Sundaram and E. Mazur, *Nat. Mater.* **1**, 217 (2002).
- ¹⁸J. Ares, T. Mancebo, and S. Bará, *Appl. Opt.* **39**, 1511 (2000).
- ¹⁹J.-M. Yi, A. Cucho, F. de León-Pérez, A. Degiron, E. Laux, E. Devaux, C. Genet, J. Alegret, L. Martín-Moreno, and T. W. Ebbesen, *Phys. Rev. Lett.* **109**, 023901 (2012).